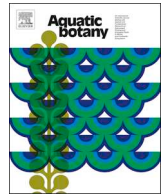




ELSEVIER

Contents lists available at ScienceDirect

Aquatic Botany

journal homepage: www.elsevier.com/locate/aquabot

Correlation of consumer grade hydroacoustic signature to submersed plant biomass



Andrew W. Howell*, Robert J. Richardson

North Carolina State University, Box 7620, Raleigh, NC, 27695, United States

ARTICLE INFO

Keywords:

Hydrilla verticillata
SAV
Echosounder
Littoral
Geographic information system
Biovolume

ABSTRACT

Invasive macrophytes, such as non-native *Hydrilla verticillata*, negatively affect lentic systems of the Southeastern United States by impeding recreational activities and power generation as well as disrupting intrinsic ecological function. Expenditures associated with aquatic weed management include costs accompanied with monitoring, mapping, and implementing control measures. Traditional biomass sampling techniques have been widely utilized to assess the extent and abundance of submersed aquatic vegetation (SAV) incursions, but often require significant labor inputs which limits repeatability, the scale of sampling, and the rapidness of processing. Advances in consumer available hydroacoustic technology and data post-processing platforms offer the opportunity to estimate SAV biomass at scale with reduced labor and economic requirements. Research was conducted at two North Carolina reservoirs to compare acoustically derived cloud-based biovolume estimations from an over-the-counter echosounder, to *in situ* hydrilla biomass measurements. Temporal patterns, spatial developments, and hydrilla biomass prediction models are presented. Biomass and biovolume measurements were positively correlated at both the Shearon Harris and Roanoke Rapids study locations. The most robust predictive equation employed generalized additive models (GAMs) from the Shearon Harris dataset which, described environmental parameters with the lowest error and greatest agreement compared to other verified models. Each biovolume to biomass relationship supported the initial hypothesis that as biovolume increases, SAV biomass increases in a positive, non-linear trend. Implications from this study may prove useful for comparing seasonal growth patterns, littoral occupancy, and herbicide treatment effects on a spatiotemporal level.

1. Introduction

Submersed aquatic vegetation (SAV) plays a vital role in contributing to whole-lake ecological assemblages by providing macroinvertebrate habitat (Strayer and Malcom, 2007), physical structure and food for shoreline fish species (Petr, 2000), and essential abiotic dynamics (Madsen et al., 2001). However, some freshwater macrophytes like the exotic species, *Hydrilla verticillata* (L.F.) Royle, present negative impacts through competition and displacement of native SAV (Van Dyke et al., 1984; Spencer and Ksander, 2000; Meadows and Richardson, 2012), and the impediment of recreational activities and power generation (Langeland, 1996). Not only can invasive macrophytes create ecologic disturbance but also economic hindrance for stakeholders. In the United States, over \$100 million is spent annually towards the management of aquatic plants (Rockwell, 2003), thus signifying the importance of monitoring infested areas and timely management application.

One measure of determining the severity of an exotic macrophyte

invasion is through *in situ* biomass sampling over time (Madsen, 1993). Using this process, aquatic plant managers also have an opportunity to identify community taxa, estimate plant abundance (Moore et al., 2000) and calculate stocking rates for grass carp (*Ctenopharyngodon idella*) (Van Dyke et al., 1984; Bonar et al., 1993). Conversely, there are several drawbacks to this method for accessing SAV. Destructive biomass sampling is an extremely laborious process (Madsen, 1999) and it can be restrictive to evaluate expansion over large spatial scales (Duarte and Kalff, 1990; Johnson and Newman, 2011). Also, spatial and temporal development of littoral plant beds may be difficult to appraise from biomass point sampling alone. However, advances in hydroacoustic technology and geographic information systems (GIS) over the last several decades offer an opportunity to estimate SAV biomass at gamut with reduced labor and economic requirements.

Numerous studies have revealed valuable implications of utilizing hydroacoustic technology for macrophyte estimation (Maceina et al., 1984; Duarte, 1987; Thomas et al., 1990; Sabol and Melton, 1996; Valley and Drake, 2005). Maceina and Shireman (1980) were the first

* Corresponding author.

E-mail address: awhowell@ncsu.edu (A.W. Howell).

<https://doi.org/10.1016/j.aquabot.2019.02.001>

Received 15 June 2018; Received in revised form 16 January 2019; Accepted 2 February 2019

Available online 04 February 2019

0304-3770/ © 2019 Published by Elsevier B.V.

investigators to recognize and document the performance of a recording fathometer (echosounder measuring depth in fathoms) to predict hydrilla biomass, although the accuracy of their regression equation was confounded by ecological growth patterns. To account for plant structure and littoral growth arrangement, Duarte (1987) successfully studied the form of macrophyte growth to create a comprehensive predictive model of submersed biomass. However, there were some limitations with this model as the echosounding transducer used was not capable of acquiring SAV less than 20 cm in height and the study site was comprised from a community of mixed species (Duarte, 1987). To overcome the structurally derived component in biomass prediction from an echosounder, Thomas et al. (1990) used biovolume, or the quantity of the water-column occupied by SAV, to indicate spatial abundance instead of complex models of plant height and form. Using biovolume as a predictor of plant structure was found to represent ecological growth habits more precise than plant bed height to quantify littoral zone development (Thomas et al., 1990). Although these researchers pioneered the use of hydroacoustic technology for predicting SAV biomass from acoustically derived signatures, there are several disadvantages from each sampling approach. Protocols commissioned by the previously described studies employed the use of scientific grade echosounders with narrow transducer beam angles (e.g. 6° to 15° beam angle) to achieve maximum SAV penetration to the benthic surface for clearer bottom detection (Maceina and Shireman, 1980; Thomas et al., 1990) and commercially available echosounding devices (e.g. 22° to 50° beam angle) to obtain a breadth of SAV profiles (Duarte, 1987; Thomas et al., 1990). Implementation of transducer beam angle extremes (e.g. 6° or 50° beam angle) limits the scope of spatially available information, inhibits the detection of short vegetation, and increases plant bed saturation loss.

Another concern is the use of mixed plant stands for the basis of regression analysis and biomass predictive models. Although Maceina and Shireman (1980) comprised their report around hydrilla, subsequent studies used a community of macrophytes to develop complex regressions between observed biomass to acoustically derived biomass projections. Therefore, a monospecific based equation should more accurately represent true biomass abundance and progression since not all SAV have the same structure to biomass ratio (Jørgensen, 2013).

Current hydroacoustic equipment and procedures are more effective than those units used to study biomass and echosounder tracings near three decades ago. Recent advances in consumer grade echosounders solve several constraints previously described, and advancements in GIS technology enable timely post-processing of survey data (Sabot et al., 2002). Modern echosounder units not only present a broader acoustic range, but also provide a cost-effective option for contiguous repeatability throughout the monitoring period (Valley et al., 2005).

The objectives of this research were to document the use of a commercially available echosounder to: 1) delineate and characterize a relationship between hydroacoustic biovolume signature to *in situ* measured hydrilla biomass; and 2) develop an algorithm for the assessment of hydrilla biomass from interpolated hydroacoustic biovolume records. From these objectives, the expected outcome is to describe a protocol for passive data acquisition while reducing the economic inputs associated with labor efforts involved in biomass collection and post-processing evaluation. In our research, a commercially available echosounding unit was utilized to correlate biomass from monospecific stands of hydrilla within two different North Carolina piedmont reservoirs using a third-party, cloud-based algorithm to aid in post-processing. We hypothesize that as hydrilla biovolume increases, biomass will increase proportionally with depth.

2. Materials and methods

Between mid-June and late-October 2015, two NC piedmont reservoirs were sampled fortnightly for hydrilla biomass and acoustically-derived SAV abundance. Timing of the boat-based sampling procedures

conformed to measurements of hydrilla growth patterns from a previous report conducted on NC lakes (Harlan et al., 1985). The two NC piedmont water bodies chosen for fixed sampling sites included Shearon Harris Reservoir (SH; Wake Co.; 35°38'0"N, 78°57'18"W) and Roanoke Rapids Lake (RR; Halifax Co.; 36°28'58.3"N, 77°43'38.7"W). These locations were selected to simulate a range of ecological factors of bathymetric profile, littoral slope, water exchange frequency, and seasonal SAV growth rates. Based on previously conducted surveys, hydrilla has been the dominant macrophyte in both reservoirs for over a decade (Nawrocki et al., 2016; NCDWQ, 2006), thus providing an optimal scenario for testing monospecific biomass correlation.

2.1. Biomass sampling

Predetermined hydrilla plots were georeferenced at both study locations prior to biomass sampling. Individual rectangular plots contained 60 sequentially numbered points (labeled 1–60), comprising a surface area of 6300 m² (50 m × 126 m) each. RR contained three plots while SH contained two plots. Points were loaded to the boat-based echosounding unit preceding the experimental period to reference biomass sampling positions.

SAV biomass was collected every two weeks at both study locations to ensure adequate temporal resolution within the sampling period for describing seasonal growth trends (Madsen, 1993). For each of the sampling periods, four randomly selected points were selected from n = 60 points per plot using a random number generator without replacement (R Core Team, 2015). These sample points were then used for all plots at both lake locations for that sampling period (i.e. SH = 8 points biweekly; RR = 12 points biweekly).

To sample SAV biomass at each of the study sites, a modified version of the boat-based vertical rake method, proposed by Johnson and Newman (2011) for macrophyte biomass collection, was utilized. The sampling rake used in this study contained eight sampling tines covering a volumetric representation of 0.25 m⁻³, affixed to a 2.5 m pole. If depth of a given collection point was greater than 2.5 m, a 3 m pole extension was added. To collect biomass within a test plot, the onboard global positioning system (GPS) from the echosounding unit was used to loiter the boat over designated random points. To increase true spatial proximity, the rake was lowered near the boat-based transducer into the water column and through the plant bed until lake bottom was reached. The rake was spun two full-rotations before slowly returning the rake back to the boat for analysis of above-benthic plant material. At the time of rake retrieval, *in situ* estimates of rake coverage and average stem length were recorded (e.g. one rake tine with macrophyte material = 12.5% coverage, two tines = 25% coverage, etc.). If any other SAV species were detected within hydrilla biomass samples (< 5% occurrence of non-hydrilla), those macrophytes were separately bagged and analyzed. All representative hydrilla biomass collected were field washed of any detritus, individually bagged for dry weight analysis, and placed in a cooler until reaching the lab.

At the lab, samples were allowed to air dry on expanded metal tables for at least 24 h prior to oven drying to reduce dehydrating time and potential decay of wet plant material. Samples were then dried at 60 °C for 48 h before biomass weights were recorded in dry biomass per unit rake volume (g dm 0.25 m⁻³).

2.2. Hydroacoustic sampling

A Lowrance HDS-7 Gen2¹ commercial grade fish-finding echosounder, with internal GPS capability of 5-Hz refresh rate and an accompanied 200-kHz single frequency transducer with 20° beam angle at 10–15 pings s⁻¹, were used to log acoustically derived SAV signatures and corresponding spatial location.

Prior to biomass sampling, a hydroacoustic scan occurred at each discrete plot, on each sampling date. Starting at the beginning of each plot, a serpentine transect with 7.5 m spacing occurred throughout the

remaining length of the plot at a boat speed of $\sim 8 \text{ km h}^{-1}$ to determine bottom area interpolation of SAV abundance at each labeled biomass sampling point. The sl2 sonar log representing a particular site location was given a unique identifier so future correlation could be prepared. All logged data were saved by the chartplotter to an internal 32GB SD memory card for further analysis and upload to ciBioBase 5.2 cloud-based software².

2.3. Data analysis

All hydroacoustic data uploaded to the ciBioBase 5.2 algorithm were exported as tabular ASCII-grid records of spatial location, biovolume percentage, and depth contour. Using similar methods to Valley et al. (2015), representative plots at all sites were imported into ESRI ArcGIS 10.2.2³ software for further post-processing and analysis. Biovolume grid-point features were transformed to shapefiles where the ArcGIS spatial analyst, feature-to-raster tool, was used to interpolate raster grids with 7.5 m^{-2} cell size. The resulting raster grids made it permissible to perform bilinear extractions of biovolume percentages to buffered hydrilla biomass point feature data collected throughout the sampling period. Using Hijmans (2015) RStudio⁴ raster package, a 2.5 m buffer was placed around each corresponding biomass point feature of interest. This buffer distance represented *in situ* spatial errors such as wind drift and GPS resolution while collecting biomass samples. The joined hydroacoustic and buffered biomass dataset attributes were then used to run correlation analysis and provide visual representation in RStudio nonparametric and ggplot2 packages (Hayfield and Racine, 2008; Wickham, 2009). Digests such as percent area covered (PAC), bathymetry, and seasonal biovolume development among plots at both SH and RR could also be statistically associated using ArcGIS and RStudio platforms. A false-positive limiting depth of 0.76 m was assigned as the minimum depth used for correlation analysis due to heavy noise and backscatter from the transducer in shallow areas (Duarte, 1987; Valley et al., 2015). Removing data points from the shallow regions in this study did not impede overall analysis as plot layouts for biomass harvesting were designed to exceed 0.76 m depths. Regression analysis and biomass prediction algorithms utilized RStudio base and non-parametric generalized additive models {mgcv} packages (Wood, 2011; R Core Team, 2015).

3. Results and discussion

3.1. Study sites and plot characteristics

Biomass was collected throughout the experimental period to represent a wide range of littoral features and seasonal variability among each test plot (Table 1). The mean seasonal biovolume percentages and biomass accumulation varied less at RR than at the SH test sites (Table 1). However, both locations had similar depth variability between individual test plots (Table 1).

Hydrilla was the only macrophyte found at SH, however, *Ceratophyllum demersum* L. (coontail), *Cabomba caroliniana* A. Gray (cabomba), and *Myriophyllum spicatum* (Eurasian watermilfoil) were found in 13 out of 71 samples at RR. Each of the three plots at RR had at least one non-hydrilla species sampled during this experiment, with plot number two containing the greatest number of non-hydrilla biomass samples. Samples which comprised > 5% of non-hydrilla biomass were identified and tested in two separate correlation analyses at RR.

3.2. Correlation of biovolume, biomass, depth and rake fullness estimations

Non-linear regression analysis was used to explain non-parametric correlations among estimated biovolume percentages and observed hydrilla biomass (Fig. 1). SH had a lower agreement (Spearman rank 'rho' = 0.51, $P < 0.001$). However, there was a strong positive trend that indicated biomass would increase with biovolume (Fig. 1a).

Table 1

Biomass and hydroacoustic sampling dynamics at each study location from 6/11/15 to 10/13/15.

Lake	Biomass Samples	Depth (m)			Seasonal Biovolume (%)		Observed Biomass (g dm^{-3})	
		Range	Mean	C.V.	Mean	C.V.	Mean	C.V.
Shearon Harris								
Plot 1	44	0.74 – 3.29	1.91	37.45	17.84	174.56	29.31	182.66
Plot 2	40	1.25 – 4.74	2.54	34.34	4.12	286.20	2.44	332.11
Roanoke Rapids								
Plot 1	19	1.11 – 2.43	1.56	22.75	79.64	30.97	40.29	121.03
Plot 2	20	1.32 – 2.96	1.92	28.06	74.53	37.45	72.50	98.43
Plot 3	19	0.88 – 2.62	1.61	39.15	64.80	47.03	52.73	135.85

Hydrilla growth at both SH test plots contained low biovolume to biomass ratios, which may explain why there was a low association when biovolume reached $\geq 25\%$ (Fig. 1a). Two correlations were comprised for RR, one with hydrilla only (Spearman rank 'rho' = 0.73, $P < 0.001$), and another with hydrilla in addition to non-hydrilla (Spearman rank 'rho' = 0.69, $P < 0.001$) (Fig. 1b). Both correlations from RR produced strong agreement and represented high biovolume to biomass ratios well; conversely, low biovolume estimates (i.e. $\leq 25\%$) were not well represented. While independent correlations from SH and RR study areas indicated positive correlations with significance, the pooled data provided the greatest explanation of association (Spearman rank 'rho' = 0.79, $P < 0.001$) (Fig. 1c). The combination of both lake data sets characterized a wide range of biovolume (0 to 100%), depth (0 to 4.74 m), and biomass (0 to 446.1 g dm), that provided well spread data and the most accurate representation of seasonal hydrilla growth. Thus, the entire range of biovolume estimates were well represented at both lake locations (Fig. 1c). Among every correlation, hydrilla biomass was often found at maximum in shallow depth localities. Overall, each biovolume to biomass relationship supports the initial hypothesis that as biovolume increases, SAV biomass should increase in a positive trend, although alterable, since bathymetry aids in delineating biovolume estimations.

With both data sets pooled, hydrilla biomass was negatively correlated to bathymetry characteristics from both study sites (Spearman rank 'rho' = -0.59, $P < 0.001$). Depth profiles of SAV had a slightly right-skewed, semi-parabolic form (Fig. 2). Average depth occurred at $\bar{x} = 2.13 \pm 0.79$ m, with biomass decreasing to either side of the maximum observed biomass value. A comparable depth to biomass correlation has also been documented by Duarte and Kalff (1990). Shallow depths limit the vertical expansion of SAV, while deeper depths do not provide as much light attenuation, due to suspended solids, to maximize SAV growth potential (Havens, 2003). This supports our ecological trend hypothesis that the majority of high biomass and biovolume was arranged within one standard deviation of the mean depth zone.

Assessing trends in biovolume distribution against known depth profiles identified non-linear relationships among all observed datasets (Fig. 3). Biovolume was influenced by depth range at both independent study sites when comparing repeated measurements of the mean biovolume percentages using Wilcoxon signed rank test (SH: $W = 48$, $P < 0.001$; RR: $W = 26$, $P < 0.001$) and also when both site datasets were combined and matched using Kruskal-Wallis rank sum test ($\chi^2 = 83.91$, $P < 0.001$) to access site specific biovolume differences. From these observations, it should be noted that SH had low biovolume percentages at all depth bins while RR best fit the high range of biovolume percentages from 1.5 to 3.0 m (Fig. 3). Therefore, the pooled

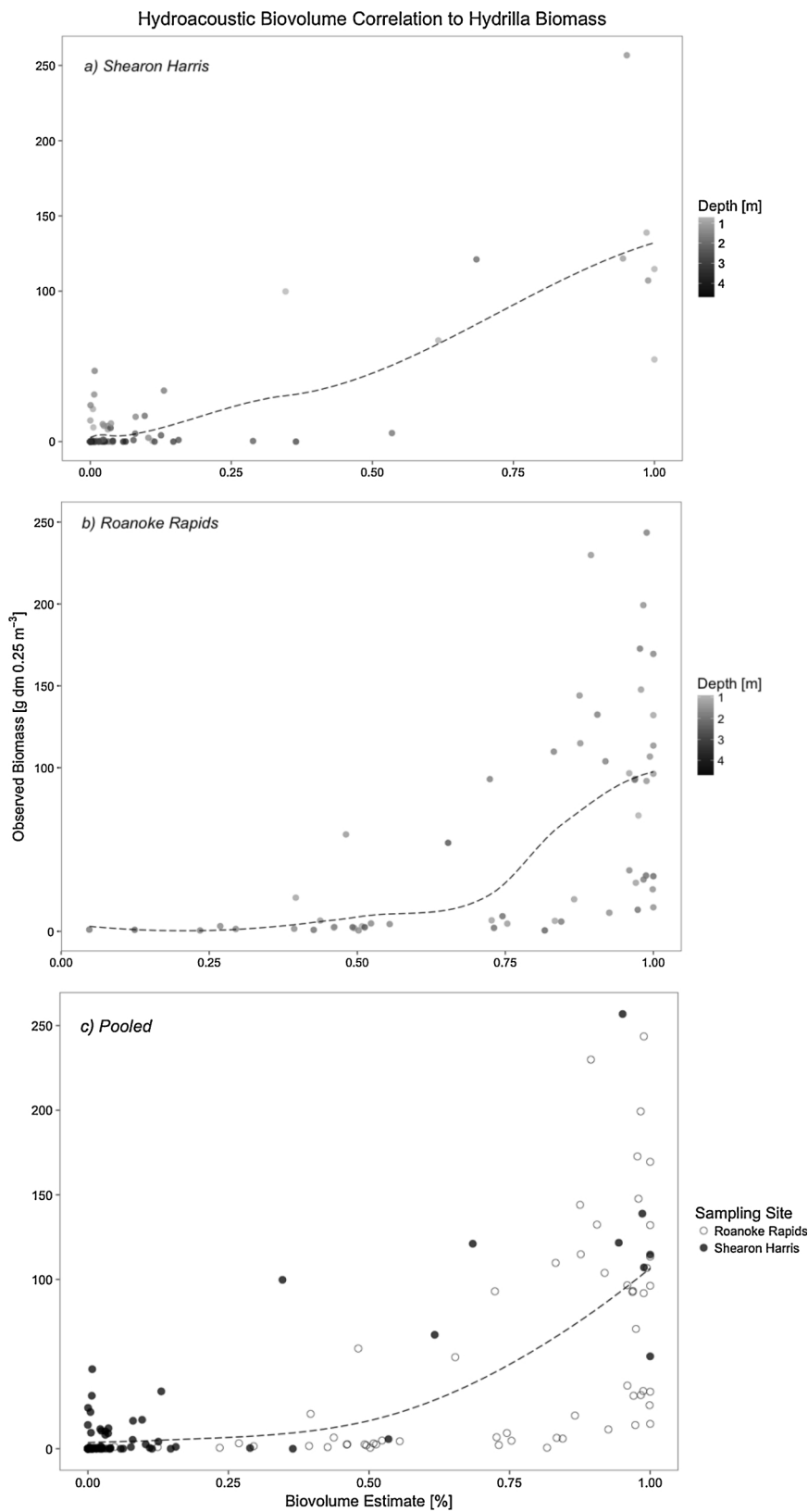


Fig. 1. a) Shearon Harris correlations among estimated biovolume percentages from ciBiobase 5.2 and observed hydrilla biomass (Spearman rank ‘rho’ = 0.51, P < 0.001). b) Roanoke Rapids correlations among estimated biovolume percentages from ciBiobase 5.2 and observed hydrilla biomass (Spearman rank ‘rho’ = 0.73, P < 0.001). c) Pooled dataset correlations among estimated biovolume percentages from ciBiobase 5.2 and observed SAV biomass by sampling locations (Spearman rank ‘rho’ = 0.79, P < 0.001). From these observations, Shearon Harris best represents data points of low biovolume and low biomass where Roanoke Rapids more clearly depicts samples containing high biovolume and high biomass.

data biovolume best represents depth bins for which water columns were fully comprised of SAV (i.e. 100% biovolume). Generally, biovolume percentages rarely exceeded 15% at depths ≥ 3.0 m. [Valley et al. \(2005\)](#) noticed an analogous trend shape in their study of depth to biovolume percentages, thus emphasizing the extent of SAV depth profiles in our experiment.

Employing non-linear modeling on rake fullness estimates, a high correlation was discovered between rake coverage and hydrilla biomass (Spearman rank ‘rho’ = 0.89). This finding is thought to be due to sampling points comprised of dense vegetation and low SAV height, or sparse vegetation with SAV capable of covering all rake tines. *in situ* plant height estimates were also found to be highly correlated to

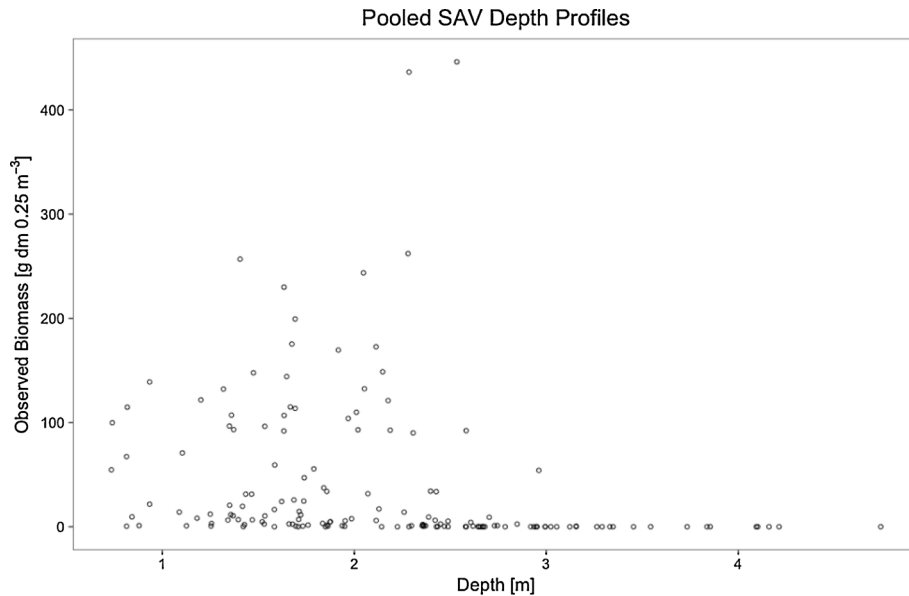


Fig. 2. Depth profiles of SAV shown have a slightly right-skewed, semi-parabolic profile. Depth average occurred at $\bar{x} = 2.13 \pm 0.79$ m, with biomass decreasing to either side of the maximum observed biomass value ($446.10 \text{ g dm } 0.25 \text{ m}^{-3}$).

collected biomass (Spearman rank ‘rho’ = 0.89), which advocates that an increase in plant height may lead to an increase in SAV biomass even in less dense stands.

3.3. Hydroacoustic biomass prediction algorithms

Multiple linear regression (MLR) and non-parametric, generalized additive models (GAM), were utilized to provide prediction equations for SH, RR, and a pooled dataset of both test sites (Tables 2 and 3). Among lake locations, the SH MLR model (Table 2a) had the greatest projected coefficient of determination ($R^2_{adj} = 0.71$, $P < 0.001$) and

the deepest littoral profile. Since depth is shown to limit the extent of vertical hydrilla growth in this study, SH thus received the highest maximum biomass estimate. Similar findings were obtained when employing GAMs, as the SH dataset provided the highest coefficient of determination ($R^2_{adj} = 0.86$, $P < 0.001$) and the lowest RMSE (129.72) among lake locations (Table 3). MLR biomass prediction for RR (Table 2b) showed lower agreement ($R^2_{adj} = 0.34$, $P < 0.001$) than SH, and GAM equations for RR had the poorest agreement ($R^2_{adj} = 0.36$, $P < 0.001$) and goodness-of-fit (Table 3). The GAM for the pooled data delivered improved model outcomes when compared to the RR dataset when cross-validated (Table 3), but pooling the data did not

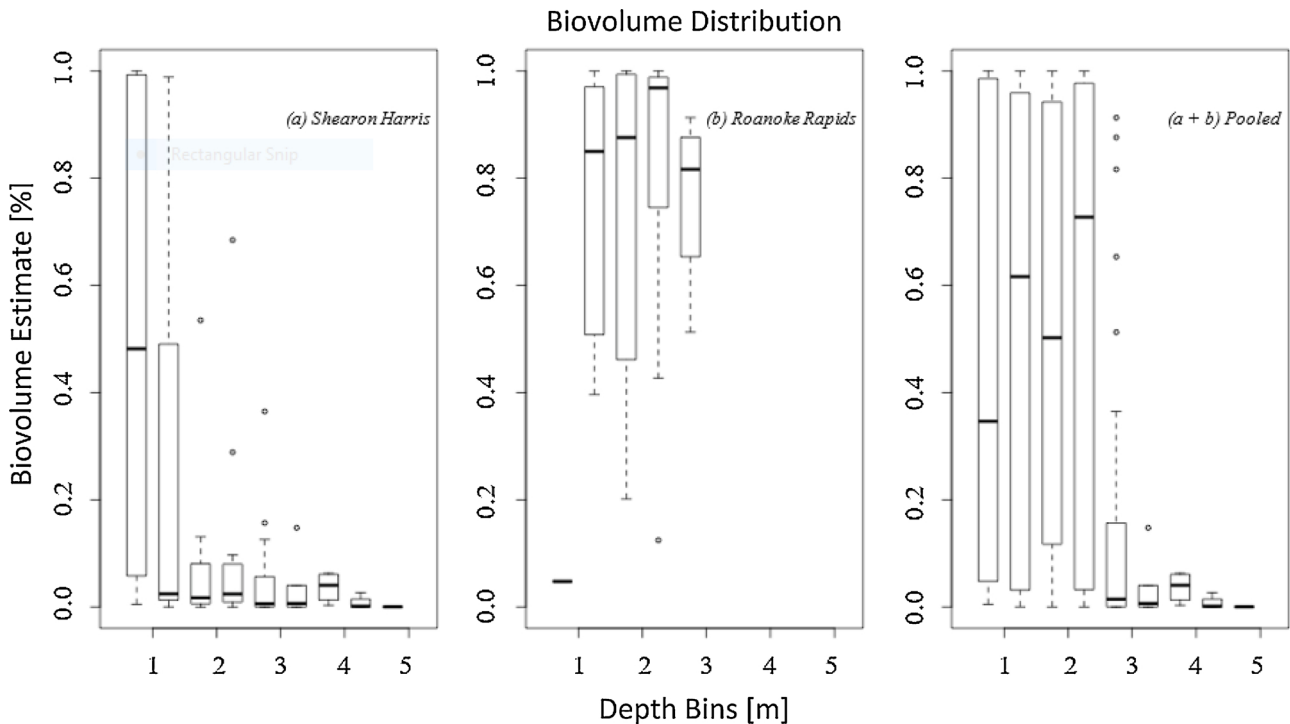


Fig. 3. Box-whisker plots of estimated biovolume detected at corresponding sampling locations at Shearon Harris, Roanoke Rapids, and a pooled dataset of both locations. Each plot depicts summary statistics of the median, the lower and upper quartiles, and the minimum and maximum biovolume values for each corresponding depth bin.

Table 2
Multiple linear regression equations comprised from either both study locations or the pooled dataset.

Lake	Mean Depth (m)	Regression Equations	DF	Prob > F	R ² _{adj}	Maximum Biomass Estimate (g) ^a
(a) Shearon Harris	2.22	DRY BIOMASS = 13.37 + 119.93 (BIOVOLUME) - 5.16 (DEPTH)	81	0.001	0.71	129.5
(b) Roanoke Rapids	1.69	DRY BIOMASS = - 22.67 + 140.46 (BIOVOLUME) - 14.50 (DEPTH)	55	0.001	0.34	98.66
(a + b) Interaction	1.91	DRY BIOMASS = 10.802 + 88.662 (BIOVOLUME) - 5.622 (DEPTH)	139	0.001	0.47	95.33

^a The highest biomass prediction at depth threshold of 0.76 m with a spatial representation of 0.25 m⁻³ using site specific training data.

provide the best explanation of biomass prediction overall. Therefore, the best-fit model identified from this study utilized GAMs from the SH dataset (*Dry Biomass* = *s*₁(*SH Biovolume*) + *s*₂(*SH Depth*) + *ti*(*SH Biovolume, SH Depth*) (Fig. 4; Table 3).

One ecological factor which occurred among the SH algorithms was the lack of data values representing high biomass and biovolume. However, the inverse relationship occurred among RR, where the low range of biomass and biovolume were not well represented. These confines were most apparent among data points containing low biomass and high biovolume. However, these issues were overcome when applying depth as a factor which homogenized the data into units of the water column occupied with SAV at given depth gradients.

From our prediction equations, many of the restraints described from previous reports have been satisfied. Following suggestions provided by Thomas et al. (1990), our algorithms utilized biovolume as the primary predictor of future biomass estimates to standardize plant height and water depth variations. Doing this defined hydrilla density among varying depths and characterized much of the ecological growth limitations documented by Maceina and Shireman (1980). Furthermore, removing any significant (*P* > 0.05) non-hydrilla biomass from the prediction models increased the accuracy of hydrilla prediction, as biomass calculations involving mixed-stands of SAV are prone to pre-eminent biomass inconsistency (Duarte, 1987).

3.4. Conclusions and management implications

Our findings are consistent with those of Stent and Hanley (1985); Duarte and Kalff (1986), and Duarte and Kalff (1990), that biomass regression analysis is a site-specific procedure due to littoral slope, turbidity, water quality, and the presence of other macrophytes. We have also shown, that even when using monospecific stands of hydrilla, there is variation of SAV biomass among discrete waterbodies. However, using GAMs to engage vigorous statistical procedures, the power of obtaining a more precise prediction model has potential for explaining environmental factors causing deviation.

A few minor limitations involving the prediction of future hydrilla biomass were apparent in this study. These disadvantages were: 1) hydrilla biomass was highly variable as biovolume reached 100% water column occupancy; 2) once biovolume reached 100%, we were unable to predict future responses in our algorithms; 3) in areas where SAV height was at the water surface, our boat was incapable of mapping those areas reliably without obstructing boat transects; and 4) we were not able to obtain biovolume estimates below 0.76 m due to transducer noise. On a cautionary note, all biomass estimations occurring when biovolume is at 100% should be double checked with depth parameters to ensure model elements are not extrapolated beyond the extent of the dataset. Also, to overcome unrepresented areas containing SAV at either depths < 0.76 m or areas containing 100% biovolume, spatial in-

Table 3
Generalized additive model (GAM) equations comprised from either both study locations or the pooled dataset.

Lake	Mean Depth (m)	Regression Equations	R ² _{adj}	Deviance Explained	RMSE	Maximum Biomass Estimate (g) ^a
(a) Shearon Harris (SH)	2.22	SH DRY BIOMASS = <i>s</i> ₁ (SH BIOVOLUME) + <i>s</i> ₂ (SH DEPTH) + <i>ti</i> (SH BIOVOLUME, SH DEPTH)	0.86	88.1%	129.72	185.0
(b) Roanoke Rapids (RR)	1.69	RR DRY BIOMASS = <i>s</i> ₁ (RR BIOVOLUME) + <i>s</i> ₂ (RR DEPTH) + <i>ti</i> (RR BIOVOLUME, RR DEPTH)	0.36	42.7%	372.74	106.9
(a + b) POOLED	1.91	POOLED DRY BIOMASS = <i>s</i> ₁ (POOLED BIOVOLUME) + <i>s</i> ₂ (POOLED DEPTH) + <i>ti</i> (POOLED BIOVOLUME, POOLED DEPTH)	0.53	55.0%	442.63	111.8

^a The highest biomass prediction at depth threshold of 0.76 m with a spatial representation of 0.25 m⁻³ using site specific training data.

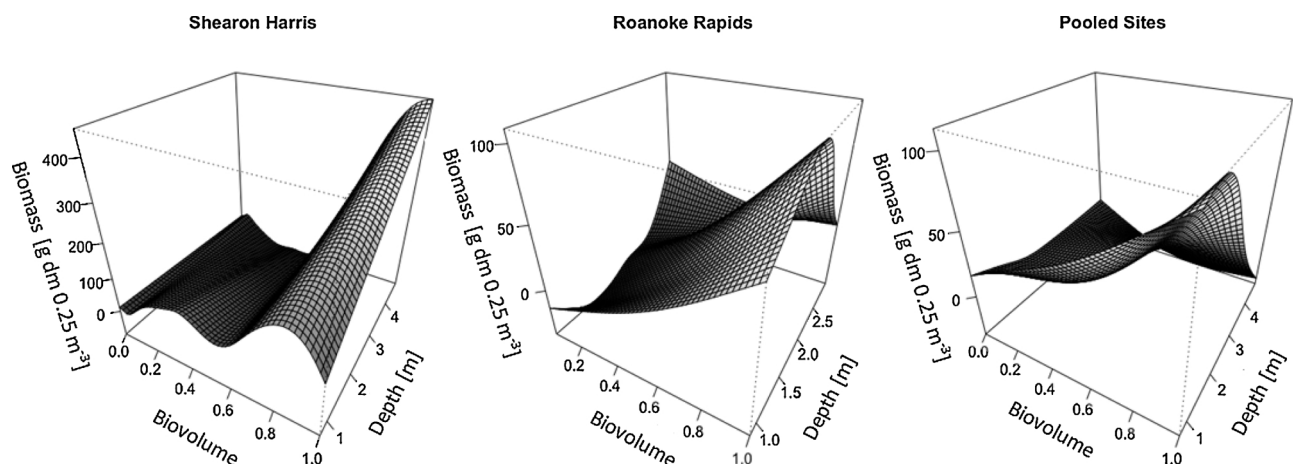


Fig. 4. Three-dimensional, perspective plots used to represent site specific biomass (Z-axis) prediction values from respective generalized additive models (GAMs).

terpolation techniques such as kriging, IDW, bilinear interpolation, or nearest neighbor may be utilized to define those regions (Valley et al., 2005).

Although some drawbacks were present with this research, the advantages of utilizing a commercially available echosounding unit for macrophyte biomass assessment are greater than the obstacles formerly described. By utilizing a third-party vendor for echosounder data management, a major reduction in post-processing time was achieved. Furthermore, our methodology proved useful in both tracking and mapping temporal changes in biovolume and biomass accumulation over time. This not only offered a repeatable, non-destructive monitoring opportunity for ecological growth patterns, but also provided visual evidence for aquatic weed management applications. Aquatic plant managers may additionally want to employ the use of the algorithms previously designated in formulating recommendations for herbicide treatments, grass carp stockings, or stakeholder reports. Since this study focused solely on hydrilla, future studies may want to validate these models in similarly structured macrophytes for biomass estimation (e.g. submersed *Myriophyllum* spp.).

In summary, our study defines the parallel between biovolume and hydrilla biomass thus stipulating technological advances used by aquatic ecologists conducting fixed point-intercept sampling protocols, while also passively recording hydrilla biomass estimation using an over-the-counter consumer echosounder.

Sources of materials

¹ Lowrance HDS-7 Gen2 chartplotter, Navico Inc., 4500 South 129th East Avenue, Suite 200, Tulsa, OK 74134.

² ciBioBase 5.2 cloud-based software, Contour Innovations, LLC, 1229 Tyler Street NE, Suite 120, Minneapolis, MN 55413.

³ ArcGIS 10.2.2, Environmental Systems Research Institute, 380 New York Street, Redlands, CA 92373.

⁴ RStudio 3.1.3, The R Foundation for Statistical Computing, 250 Northern Ave, Boston, MA 02210.

Acknowledgments

The authors would like to acknowledge the efforts of the NCSU Aquatic Weed Science Laboratory for their assistance with data collection, especially, Steve Hoyle and Stephanie Nawrocki. An appreciation is also extended to Rachel West for her statistical consultation, and Brett Hartis, Stacy Nelson, Erin Hestir, Wesley Everman, and David Jordan for their contribution of technical assistance throughout this research and manuscript review. This research was made possible with partial funding through the NCSU Cross-College Enrichment Grant Program.

References

- Bonar, S.A., Thomas, G.L., Thiesfeld, S.L., Pauley, G.B., Stables, T.B., 1993. Effect of triploid grass carp on the aquatic macrophyte community of Devils Lake, Oregon. *N. Am. J. Fish. Manag.* 13, 757–765.
- Duarte, C.M., 1987. Use of echosounder tracings to estimate the aboveground biomass of submerged plants in lakes. *Can. J. Fish. Aquat. Sci.* 44, 732–735.
- Duarte, C.M., Kalff, J., 1986. Littoral slope as a predictor of the maximum biomass of submerged macrophyte communities. *Limnol. Oceanogr.* 31, 1072–1080.
- Duarte, C.M., Kalff, J., 1990. Patterns in the submerged macrophyte biomass of lakes and the importance of the scale of analysis in the interpretation. *Can. J. Fish. Aquat. Sci.* 47, 357–363.
- Harlan, S.M., Davis, G.J., Pesacreta, F.J., 1985. Hydrilla in Three North Carolina Lakes. *J. Aquat. Plant Manag.* 23, 68–71.
- Havens, K.E., 2003. Submersed aquatic vegetation correlations with depth and light

- attenuating materials in a shallow subtropical lake. *Hydrobiologia.* 493, 173–186.
- Hayfield, T., Racine, J.S., 2008. Nonparametric econometrics: the *np* package. *J. Stat. Software* 27, 5. <http://www.jstatsoft.org/v27/i05/>.
- Hijmans, R.J., 2015. raster: Geographic Data Analysis and Modeling. 5-2. R package version 2. <http://cran.r-project.org/package=raster>.
- Jørgensen, S.E., 2013. Handbook of Environmental Data and Ecological Parameters, 1st edition. Pergamon 1210 pp.
- Johnson, J.A., Newman, R.M., 2011. A comparison of two methods for sampling biomass of aquatic plants. *J. Aquat. Plant Manag.* 49, 1–8.
- Langeland, K.A., 1996. *Hydrilla verticillata* (L.F.) Royle (Hydrocharitaceae), the perfect aquatic weed. *Castanea* 61, 293–304.
- Maceina, M.J., Shireman, J.V., 1980. The use of a recording fathometer for determination of distribution and biomass of hydrilla. *J. Aquat. Plant Manag.* 18, 34–39.
- Maceina, M.J., Shireman, J.V., Langeland, K.A., Canfield Jr., D.E., 1984. Prediction of submersed plant biomass by use of a recording fathometer. *J. Aquat. Plant Manag.* 22, 35–38.
- Madsen, J.D., 1993. Biomass techniques for monitoring and assessing control of aquatic vegetation. *Lake Reservoir Manage. J.* 7, 141–154.
- Madsen, J.D., 1999. Point Intercept and Line Intercept Methods for Aquatic Plant Management. APCRP Technical Notes Collection (TN APCRP-M1-02). U.S. Army Engineer Research and Development Center, Vicksburg, MS, pp. 1–17.
- Madsen, J.D., Chambers, P.A., James, W.F., Kock, E.W., Westlake, D.F., 2001. The interaction between water movement, sediment dynamics and submersed macrophytes. *Hydrobiologia* 444, 71.
- Meadows, S.T., Richardson, R.J., 2012. Competition of monoecious hydrilla with other submersed macrophytes. Abstract. Proceedings of the 52nd Annual Meeting Aquatic Plant Management Society (APMS).
- Moore, K.A., Wilcox, D.J., Orth, R.J., 2000. Analysis of the abundance of submersed aquatic vegetation communities in the Chesapeake Bay. *Estuaries* 23, 115–127.
- Nawrocki, J.J., Richardson, R.J., Hoyle, S.T., 2016. Monoecious hydrilla tuber dynamics following various management regimes on four North Carolina reservoirs. *J. Aquat. Plant Manag.* 54, 12–19.
- NCDWQ: NC Department of Environment and Natural Resources: Division of Water Quality, 2006. Total Maximum Daily Load for Aquatic Weeds for Rockingham City Lake, Roanoke Rapids Lake, Big Lake, Reedy Creek Lake, and Lake Wackena in North Carolina. pp. 1–53.
- Petr, T., 2000. Interactions Between Fish and Aquatic Macrophytes in Inland Waters. A Review. FAO fisheries technical paper. FAO, Rome, Italy 396, 185p.
- R Core Team, 2015. R: a Language and Environment for Statistical Computing. R Foundation for Statistical Computing, Vienna, Austria. <http://www.R-project.org/>.
- Rockwell, W.H., 2003. Summary of a Survey of the Literature on the Economic Impact of Aquatic Weeds. Report to the Aquatic Ecosystem Restoration Foundation. pp. 1–18.
- Sabol, B.M., Melton Jr., R.E., 1996. Development of an Automated System for Detection and Mapping of Submersed Aquatic Vegetation With Hydroacoustic and Global Positioning System Technologies; Report 1: the Submersed Aquatic Vegetation Early Warning System (SAVEWS)-System Description and User's Guide (Version 1.0). Joint Agency Guntersville Project Aquatic Plant Management, TVA/WR-95-00. Tennessee Valley Authority, Knoxville, Tennessee.
- Sabol, B., Melton Jr., R.E., Chamberlain, R., Doering, P., Haurert, K., 2002. Evaluation of a digital echo sounder system for detection of submersed aquatic vegetation. *Estuaries* 25, 133–141.
- Spencer, D.F., Ksander, G.G., 2000. Interactions between American pondweed and monoecious hydrilla grown in mixtures. *J. Aquat. Plant Manag.* 38, 5–13.
- Stent, C.J., Hanley, S., 1985. A recording echo sounder for assessing submerged aquatic plant populations in shallow lakes. *Aquat. Bot.* 21, 377–394.
- Strayer, D.L., Malcom, H.M., 2007. Submersed vegetation as habitat form invertebrates in the Hudson River estuary. *Estuaries Coasts* 30, 253–264.
- Thomas, G.L., Thiesfeld, S.L., Bonar, S.A., Crittenden, R.N., Pauley, G.B., 1990. Estimation of submergent plant bed biovolume using acoustic range information. *Can. J. Fish. Aquat. Sci.* 47, 805–812.
- Valley, R.D., Drake, M.T., 2005. Accuracy and precision of hydroacoustic estimates of aquatic vegetation and the repeatability of whole-lake surveys: field tests with a commercial echosounder. Minnesota Department of Natural Resources: Investigational Report. 527. pp. 1–12.
- Valley, R.D., Drake, M.T., Anderson, C.S., 2005. Evaluation of alternative interpolation techniques for the mapping of remotely-sensed submersed vegetation abundance. *Aquat. Bot.* 81, 13–25.
- Valley, R.D., Johnson, M.B., Dustin, D.L., Jones, K.D., Lauenstein, M.R., Nawrocki, J., 2015. Combining hydroacoustic and point-intercept survey methods to assess aquatic plant species abundance patterns and community dominance. *J. Aquat. Plant Manag.* 53, 121–129.
- Van Dyke, J.M., Leslie Jr., A.J., Nall, L.E., 1984. The effects of the grass carp on aquatic macrophytes of four Florida lakes. *J. Aquat. Plant Manag.* 22, 87–95.
- Wickham, H., 2009. ggplot2: Elegant Graphics for Data Analysis. Springer-Verlag, New York. <https://cran.r-project.org/web/packages/ggplot2/index.html>.
- Wood, S.N., 2011. Fast stable restricted maximum likelihood and marginal likelihood estimation of semiparametric generalized linear models. *J. R. Stat. Soc. Ser. B* 73, 3–36.